

Symmetry energy at supra-saturation densities via the Gravitational Waves from GW170817

Hui Tong,¹ Peng-Wei Zhao,¹ and Jie Meng^{1,2,3}

¹*State Key Laboratory of Nuclear Physics and Technology,
School of Physics, Peking University
Beijing 100871, China*

²*Department of Physics, University of Stellenbosch, Stellenbosch, South Africa*

³*Yukawa Institute for Theoretical Physics,
Kyoto University, Kyoto 606-8502, Japan*

Abstract

Motivated by the historical detection of gravitational waves from GW170817, the neutron star and the neutron drop, i.e., a certain number of neutrons confined in an external field, are systematically investigated by *ab initio* calculations as well as the nonrelativistic and relativistic state-of-art density functional theories. Strong correlations are found among the neutron star tidal deformability, the neutron star radius, the root-mean-square radii of neutron drops, and the symmetry energies of nuclear matter at supra-saturation densities. From these correlations and the upper limit on the tidal deformability extracted from GW170817, the neutron star radii, the neutron drop radii, and the symmetry energy at twice saturation density are respectively constrained as $R_{1.4M_{\odot}} \leq 12.94$ km, $R_{\text{nd}} \leq 2.36$ fm, and $E_{\text{sym}}(2\rho_0) \leq 53.2$ MeV.

On August 17, 2017, a gravitational wave (GW) signal from a merger of binary neutron star (BNS) system was observed by the advanced LIGO and Virgo Collaborations for the first time, i.e., GW170817 [1]. This observation, together with the followed observation of the associated electromagnetic emissions [2, 3], has opened a significant multimessenger era in the field of astrophysics and nuclear physics. In particular, the GW signal provides a crucial opportunity to investigate the properties of the compact matter—neutron star.

According to the GW170817 signal from the merger of BNS, one can extract the masses of neutron stars. The measured chirp mass [4] is $\mathcal{M} = 1.188_{-0.002}^{+0.004} M_{\odot}$ [1], which is defined as $\mathcal{M} = (M_1 M_2)^{3/5} (M_1 + M_2)^{-1/5}$, from the component masses M_1 and M_2 . In addition, the tidal deformability Λ can also be extracted, which represents the mass quadrupole moment response of a neutron star to the strong gravitational field induced by its companion. The tidal deformability of a neutron star is defined as $\Lambda = \frac{2}{3} k_2 \left(\frac{c^2 R}{GM} \right)^5$, where k_2 is the second Love number, M and R are the neutron star mass and radius, c and G are the speed of light and the gravitational constant, respectively [5–9]. Therefore, the tidal deformability is expected to have a high sensitivity to the neutron star radius ($\Lambda \sim R^5$). For a neutron star with mass $1.4 M_{\odot}$, the LIGO and Virgo collaborations provided an upper limit $\Lambda_{1.4 M_{\odot}} \leq 580$ with a credible level of 90% [10].

Both the mass and tidal deformability of neutron stars provide new opportunities to study the equation of state (EOS) for nuclear matter [11, 12]. In particular, its isovector properties, e.g., symmetry energy, play a significant role in exploring new physics in both nuclear physics and astrophysics. By adopting the tidal deformability limit from the GW signal, the neutron star radius as well as the neutron skin thickness of ^{208}Pb , which is strongly correlated to the slope of the symmetry energy L at nuclear matter saturation density ($\rho_0 \approx 0.16 \text{ fm}^{-3}$), have been inferred [13]. A direct relation between the tidal deformability and L has been studied in Refs. [14, 15]. However, both works indicate that the tidal deformability, which probes the symmetry energy at around twice saturation density, may not provide a strong constraint on the nuclear matter bulk parameters at the saturation density.

A neutron drop system is very useful to probe the high-density behavior of nuclear matter. The neutron drop is a novel inhomogeneous pure neutron system consisting of a few neutrons confined in an external field. By varying the number of neutrons and/or the strength of the external field for neutron drops, one can obtain a variety of information for the drops at various densities. The nuclear EOS ranging from lower densities to higher densities could

be correlated to the neutron drop properties [16].

An accurate knowledge of the neutron drop properties is crucial to understand the physics of neutron stars [17–19] and to probe possible new physics for nuclei with large isospin in as yet unexplored regions of the nuclear chart [20]. Due to its simplicity, the neutron drop is widely used to test various nuclear many-body techniques, e.g., *ab initio* approaches for light nuclei and density functional theories (DFTs) for heavy ones [16, 21–28]. The former are based on realistic nucleon-nucleon (NN) and three-nucleon ($3N$) interactions with a many-body Hamiltonian, while the latter depend on a variation of an energy functional with respect to nucleon densities.

Therefore, it is timely and interesting to link the GW signals to the nuclear EOS and the neutron drop properties, so as to promote both the nuclear physics and the astrophysics with the advent of the multi-messenger era.

In this Letter, the neutron star tidal deformability and its correlation with the neutron star radius are systematically investigated with the state-of-art DFTs [29–32] and the *ab initio* relativistic Brueckner-Hartree-Fock (RBHF) theory [33–35]. A strong linear correlation between the root-mean-square (rms) radii of neutron drops and the neutron star radii is demonstrated. Furthermore, a strong correlation between the symmetry energy at twice saturation density and the neutron drop radii is illustrated. With these correlations, the upper limit of the tidal deformability $\Lambda_{1.4M_\odot} \leq 580$ [10] extracted from GW170817 is used to constrain the rms radii of neutron drops and, in turn, the symmetry energies of nuclear matter at supra-saturation densities.

In the context of GW170817, the tidal deformabilities Λ_1 and Λ_2 associated with the high mass M_1 and low mass M_2 components of the BNS are calculated by a series of DFTs and the *ab initio* RBHF theory. As shown in Fig. 1, the calculations here are carried out by many well-determined density functionals widely used for nuclear and astrophysical physics. In particular, the EOSs here are consistent with the observed lower bound on the maximum mass of neutron stars for $M_{\text{max}} > 2M_\odot$ [36, 37]. The adopted DFTs range from nonrelativistic models (e.g., SLy4 and those starting with S) [38], to relativistic models with the nonlinear meson exchange functionals (NL models, PK1, TM1), as well as the density-dependent meson exchange ones (DD-ME and RHF models, PKDD, TW99) [39, 40]. *Ab initio* calculations have been carried out with the RBHF theory using the Bonn potentials [35]. Note that the *ab initio* variational calculations (APR) are also shown for

comparison [41].

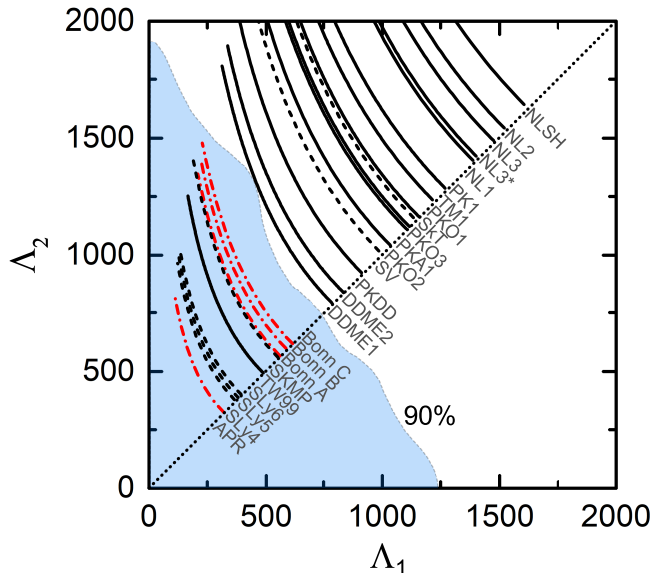


FIG. 1. (Color online.) Tidal deformabilities Λ_1 and Λ_2 associated with the high mass M_1 and low mass M_2 components of the binary neutron star obtained by a set of relativistic (solid lines), non-relativistic (dashed lines) density functionals, and the results from *ab initio* Relativistic Brueckner-Hartree-Fock (RBHF) theory using the Bonn potentials and the *ab initio* variational calculations (APR) [41] (dot-dashed lines). The boundary of $\Lambda_1 = \Lambda_2$ is denoted by the diagonal dotted line. The 90% probability contour is extracted from GW170817 [10].

Allowing a variation of the high mass M_1 within the range $1.365M_\odot \leq M_1 \leq 1.60M_\odot$, the corresponding low mass M_2 can be determined by the chirp mass $\mathcal{M} = (M_1 M_2)^{3/5} (M_1 + M_2)^{-1/5} = 1.188M_\odot$ given by GW170817 [1], and one can then obtain the relations between Λ_1 and Λ_2 of a BNS. As a comparison, we also plot the latest 90% probability contour recommended by the LIGO and Virgo observatories with the low-spin priors [10]. Since the isovector channels of the density functionals shown in Fig. 1 are loosely determined in the fitting procedures, their predictions span a fairly wide range of tidal deformabilities Λ . For a given neutron star mass, the functionals with a softer (stiffer) symmetry energy yield smaller (larger) stellar radii and correspondingly smaller (larger) tidal deformabilities. One can see that the curves locating on the right side of the contour are ruled out by GW170817. This indicates that overly stiff EOSs, which produce large values of Λ and correspondingly large radii for fixed M are disfavored by the GW170817. Nevertheless, the *ab initio* calculations

and a relatively large set of EOSs situate inside the 90% probability contour.

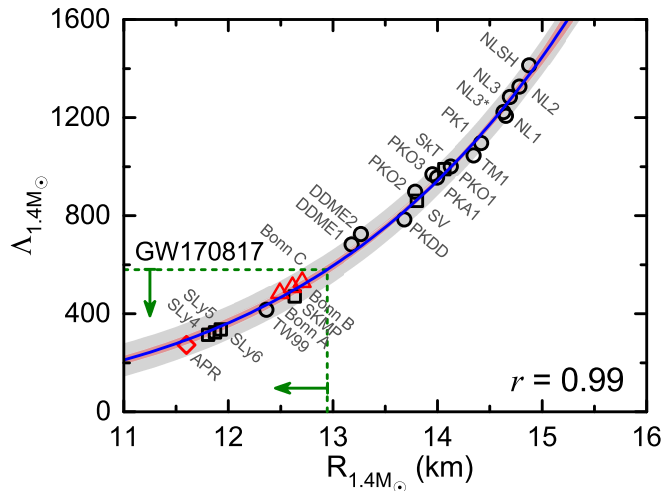


FIG. 2. (Color online) The tidal deformability $\Lambda_{1.4M_\odot}$ of a $1.4M_\odot$ neutron star as a function of the corresponding radius $R_{1.4M_\odot}$ (km) as predicted by various relativistic (circles) and nonrelativistic (squares) density functionals, in comparison with results calculated by RBHF theory using the Bonn potentials (triangles) and the *ab initio* variational calculations (APR, diamond). The blue curve line is the fit to the results of density functionals, and the inner (outer) colored regions depict the 95% confidence (prediction) intervals of the curvilinear regression. The vertical arrow indicates the constraint $\Lambda_{1.4M_\odot} \leq 580$ [10] from GW170817, which leads to $R_{1.4M_\odot} \leq 12.94$ km labeled by the horizontal arrow according to the correlations.

The tidal deformabilities predicted by both relativistic and nonrelativistic DFTs are very useful to extract the correlations between the tidal deformabilities and other isovector-sensitive properties. The correlations between the tidal deformability $\Lambda_{1.4M_\odot}$ and the radius $R_{1.4M_\odot}$ of a neutron star with mass $M = 1.4M_\odot$ are shown in Fig. 2. The predictions of DFTs are fitted by the equation $\Lambda_{1.4M_\odot} = aR_{1.4M_\odot}^b$ with $a \approx 7.29 \times 10^{-5}(\text{km}^{-b})$ and $b \approx 6.21$. A strong correlation between $\Lambda_{1.4M_\odot}$ and $R_{1.4M_\odot}$ with a correlation coefficient of $r \approx 0.99$ is revealed.

It is important to underscore that this strong correlation between $\Lambda_{1.4M_\odot}$ and $R_{1.4M_\odot}$ is universal since it is based on widely different nuclear density functionals. Furthermore, the correlation predicted by DFTs is supported by the *ab initio* calculations including the RBHF theory and the APR, as shown in Fig. 2. The universal correlation between $\Lambda_{1.4M_\odot}$ and $R_{1.4M_\odot}$ allows one to extract $R_{1.4M_\odot}$ from the tidal deformability. From GW170817, the

result $\Lambda_{1.4M_\odot} \leq 580$ [10] leads to $R_{1.4M_\odot} \leq 12.94$ km. This is consistent with other works, such as $R_{1.4M_\odot} \leq 13.76$ km [13] and $R_{1.4M_\odot} \leq 13.6$ km [42] from the tidal deformability [1], and $R_{1.4M_\odot} \leq 13.6$ km from the available terrestrial laboratory data [43].

The neutron drop is an inhomogeneous pure neutron system consisting of a few neutrons confined in an external field. Although the radius of a neutron drop is smaller than that of a neutron star by 19 orders of magnitude, both quantities highly depend on the symmetry energy [16, 44–46]. Therefore, it is interesting to investigate the correlations between them.

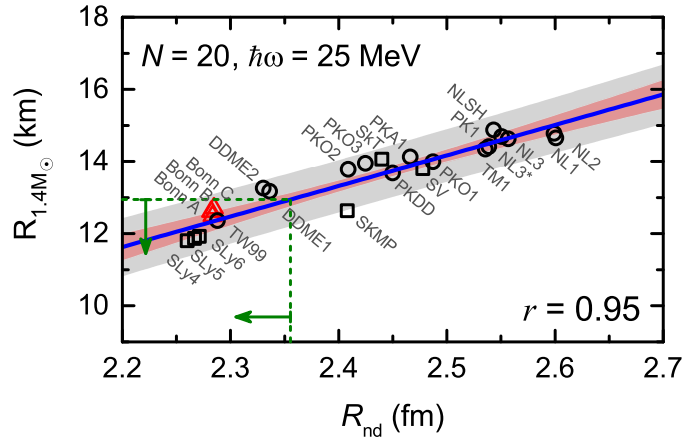


FIG. 3. (Color online) The radius of a $1.4M_\odot$ neutron star against the root-mean-square (rms) radius R_{nd} for $N = 20$ neutrons trapped in a HO potential ($\hbar\omega = 25$ MeV) obtained with various relativistic (circles) and nonrelativistic (squares) density functionals, as well as the RBHF theory using the Bonn potentials (triangles). The blue line is a linear fit to the results of density functionals. The upper limit $R_{1.4M_\odot} \leq 12.94$ km deduced from Fig. 2 is shown with the vertical arrow, which gives a constraint $R_{\text{nd}} \leq 2.36$ fm labeled by the horizontal arrow.

In Fig. 3, the radius of a $1.4M_\odot$ neutron star and the rms radius R_{nd} for $N = 20$ neutrons confined in a harmonic oscillator (HO) potential ($\hbar\omega = 25$ MeV) calculated with relativistic and nonrelativistic DFTs and the *ab initio* RBHF theory are given. The DFTs predictions for $R_{1.4M_\odot}$ and R_{nd} respectively range from 11.5 km to 15.0 km, and from 2.25 fm to 2.60 fm, due to their differences in the isovector channels.

A strong linear correlation can be established between the neutron star radius $R_{1.4M_\odot}$ and the rms radius of the neutron drop R_{nd} by fitting the results from DFTs. The Pearson's correlation coefficient is $r = 0.95$. This linear correlation between $R_{1.4M_\odot}$ and R_{nd} is universal with the neutron number and the strength of the external field for the neutron drops, as

long as the central density of the drop is comparable with that of the neutron stars, i.e., around 2–3 times saturation density.

The correlation between $R_{1.4M_\odot}$ and R_{nd} predicted by DFTs is supported by the *ab initio* RBHF calculations. The verification of this linear correlation from *ab initio* calculations gives us confidence to deduce $R_{\text{nd}} \leq 2.36$ fm from $R_{1.4M_\odot} \leq 12.94$ km obtained with the $\Lambda_{1.4M_\odot}$ vs $R_{1.4M_\odot}$ relation in Fig. 2. With the future high-accuracy GW measurements, the constraints on the radii of neutron drops would be accurately deduced, which might provide a useful constraint for three-neutron forces [16].

Apart from the constraint from GW170817, the correlation can also be used in combination with other astronomical observations. For example, the future precise radii of neutron stars from photospheric radius expansion X-ray bursts and quiescent low-mass X-ray binaries [47, 48] can provide a similar constraint on the neutron drop radii.

By changing the strength of the external field, the neutron drop system with a central density up to 3 times saturation density can be obtained, which is very useful to probe the symmetry energy at high density.

The symmetry energy at the density ρ is defined as $E_{\text{sym}}(\rho) = \frac{1}{2} \frac{\partial^2 E(\rho, \alpha)}{\partial \alpha^2} \Big|_{\alpha=0}$, where $E(\rho, \alpha)$ is the binding energy per nucleon and the asymmetry parameter $\alpha = \frac{\rho_n - \rho_p}{\rho}$ with the proton densities ρ_p and the neutron densities ρ_n . The density dependence of the nuclear symmetry energy is essential to understand both finite nuclei and neutron stars. However, the constraints on the density dependence of the symmetry energy either from the experiment of the heavy ion collisions [49] or the predictions from variant models [50] have large ambiguity.

In Fig. 4, the symmetry energy of nuclear matter at twice saturation density $E_{\text{sym}}(2\rho_0)$ and the rms radii R_{nd} of 20 neutrons in a HO with $\hbar\omega = 25$ MeV calculated by DFTs are given. A strong correlation can be established between $E_{\text{sym}}(2\rho_0)$ and the neutron drop radius R_{nd} . The Pearson's coefficient by fitting the DFTs results is $r = 0.96$. It demonstrates that a precise determination of the neutron drop radii could set a basic constraint on the symmetry energy at twice saturation density. The constraint $R_{\text{nd}} \leq 2.36$ fm in Fig. 3 yields $E_{\text{sym}}(2\rho_0) \leq 53.2$ MeV.

The constraint on the symmetry energy $E_{\text{sym}}(2\rho_0) \leq 53.2$ MeV is consistent with the recent ASY-EOS experimental results $50.8 \text{ MeV} \leq E_{\text{sym}}(2\rho_0) \leq 60.4 \text{ MeV}$ [51] and the predictions by *ab initio* RBHF theory. Accordingly, the ambiguity of the symmetry energy predicted at twice saturation density is remarkably reduced. The present results provide an

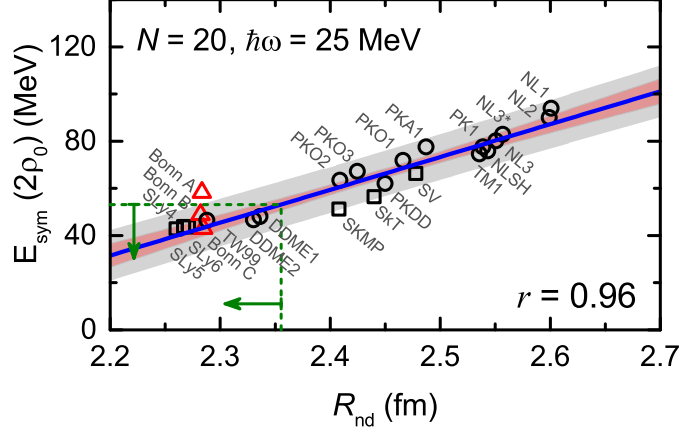


FIG. 4. (Color online) Correlations between the symmetry energy of nuclear matter at twice nuclear saturation density and rms radii of 20 neutrons in a HO with $\hbar\omega = 25$ MeV, calculated by relativistic (circles), nonrelativistic (squares) density functional theories and *ab initio* methods (triangles). The upper limit $R_{\text{nd}} \leq 2.36$ fm deduced from the correlations between $R_{1.4}$ vs R_{nd} is shown with the horizontal arrow, which gives rise to an upper limit $E_{\text{sym}}(2\rho_0) \leq 53.2$ MeV labeled by the vertical arrow.

excellent agreement between the astrophysical GW observations and the terrestrial experiments, and reveal a soft symmetry energy in the regime of high density.

Similar correlations between R_{nd} and $E_{\text{sym}}(\rho)$ for $\rho = \rho_0 \sim 4\rho_0$ have been analyzed. The symmetry energies from $E_{\text{sym}}(2\rho_0)$ to $E_{\text{sym}}(3\rho_0)$ are correlated with R_{nd} in a linear way with the Pearson's coefficient $r \sim 0.96$. Such a connection should be reasonable because the central density of the neutron drop with 20 neutrons confined in a HO potential with $\hbar\omega = 25$ MeV is around and even slightly larger than the twice saturation density. Although there is no data for the symmetry energy beyond the twice saturation density, the obtained constraints on $E_{\text{sym}}(\rho)$ for $\rho = 2\rho_0 \sim 3\rho_0$ from R_{nd} are supported by the *ab initio* RBHF and APR calculations [41].

In summary, the neutron star and the neutron drop have been systematically investigated by *ab initio* calculations as well as the state-of-art DFTs. Strong correlations are found among the neutron star tidal deformability, the neutron star radius, the root-mean-square radii of neutron drops, and the symmetry energies of nuclear matter at supra-saturation densities. From these correlations and the tidal deformability extracted from GW170817, the neutron star radii, the neutron drop radii, and the symmetry energy at twice saturation

density are respectively constrained as $R_{1.4M_{\odot}} \leq 12.94$ km, $R_{\text{nd}} \leq 2.36$ fm, and $E_{\text{sym}}(2\rho_0) \leq 53.2$ MeV. With the advent of the multi-messenger era, the present work would have an enduring impact on understanding the neutron-rich systems and nuclear EOS with the GW signals.

This work was partly supported by the National Key R&D Program of China (Contract No. 2017YFE0116700 and No. 2018YFA0404400) and the National Natural Science Foundation of China (NSFC) under Grants No. 11335002, No. 11621131001.

-
- [1] B. Abbott *et al.* (LIGO Scientific Collaboration and Virgo Collaboration), *Phys. Rev. Lett.* **119**, 161101 (2017).
 - [2] V. Savchenko *et al.*, *Astrophys. J. Lett.* **848**, L15 (2017).
 - [3] A. Goldstein *et al.*, *Astrophys. J. Lett.* **848**, L14 (2017).
 - [4] P. C. Peters and J. Mathews, *Phys. Rev.* **131**, 435 (1963).
 - [5] T. Damour, M. Soffel, and C. Xu, *Phys. Rev. D* **45**, 1017 (1992).
 - [6] T. Hinderer, *Astrophys. J.* **677**, 1216 (2008).
 - [7] E. E. Flanagan and T. Hinderer, *Phys. Rev. D* **77**, 021502 (2008).
 - [8] T. Damour and A. Nagar, *Phys. Rev. D* **80**, 084035 (2009).
 - [9] S. Postnikov, M. Prakash, and J. M. Lattimer, *Phys. Rev. D* **82**, 024016 (2010).
 - [10] B. Abbott *et al.* (LIGO Scientific Collaboration and Virgo Collaboration), *Phys. Rev. Lett.* **121**, 161101 (2018).
 - [11] J. M. Lattimer and M. Prakash, *Science* **304**, 536 (2004).
 - [12] J. M. Lattimer and M. Prakash, *Phys. Rep.* **621**, 127 (2016), memorial Volume in Honor of Gerald E. Brown.
 - [13] F. J. Fattoyev, J. Piekarewicz, and C. J. Horowitz, *Phys. Rev. Lett.* **120**, 172702 (2018).
 - [14] Y. Lim and J. W. Holt, *Phys. Rev. Lett.* **121**, 062701 (2018).
 - [15] T. Malik, N. Alam, M. Fortin, C. Providência, B. K. Agrawal, T. K. Jha, B. Kumar, and S. K. Patra, *Phys. Rev. C* **98**, 035804 (2018).
 - [16] P. W. Zhao and S. Gandolfi, *Phys. Rev. C* **94**, 041302 (2016).
 - [17] D. G. Ravenhall, C. J. Pethick, and J. R. Wilson, *Phys. Rev. Lett.* **50**, 2066 (1983).
 - [18] E. F. Brown and A. Cumming, *Astrophys. J.* **698**, 1020 (2009).

- [19] M. Buraczynski and A. Gezerlis, Phys. Rev. Lett. **116**, 152501 (2016).
- [20] J. Erler, N. Birge, M. Kortelainen, W. Nazarewicz, E. Olsen, A. M. Perhac, and M. Stoitsov, Nature **486**, 509 (2012).
- [21] B. S. Pudliner, A. Smerzi, J. Carlson, V. R. Pandharipande, S. C. Pieper, and D. G. Ravenhall, Phys. Rev. Lett. **76**, 2416 (1996).
- [22] S. Gandolfi, J. Carlson, and S. C. Pieper, Phys. Rev. Lett. **106**, 012501 (2011).
- [23] S. K. Bogner, R. J. Furnstahl, H. Hergert, M. Kortelainen, P. Maris, M. Stoitsov, and J. P. Vary, Phys. Rev. C **84**, 044306 (2011).
- [24] P. Maris, J. P. Vary, S. Gandolfi, J. Carlson, and S. C. Pieper, Phys. Rev. C **87**, 054318 (2013).
- [25] H. D. Potter, S. Fischer, P. Maris, J. P. Vary, S. Binder, A. Calci, J. Langhammer, and R. Roth, Phys. Lett. B **739**, 445 (2014).
- [26] J. Carlson, S. Gandolfi, F. Pederiva, S. C. Pieper, R. Schiavilla, K. E. Schmidt, and R. B. Wiringa, Rev. Mod. Phys. **87**, 1067 (2015).
- [27] S. Shen, H. Liang, J. Meng, P. Ring, and S. Zhang, Phys. Rev. C **97**, 054312 (2018).
- [28] S. Shen, H. Liang, J. Meng, P. Ring, and S. Zhang, Phys. Lett. B **778**, 344 (2018).
- [29] P. Ring, Prog. Part. Nucl. Phys. **37**, 193 (1996).
- [30] M. Bender, P.-H. Heenen, and P.-G. Reinhard, Rev. Mod. Phys. **75**, 121 (2003).
- [31] D. Vretenar, A. V. Afanasjev, G. A. Lalazissis, and P. Ring, Phys. Rep. **409**, 101 (2005).
- [32] J. Meng, *Relativistic Density Functional for Nuclear Structure* (WORLD SCIENTIFIC, 2016).
- [33] P. G. Krastev and F. Sammarruca, Phys. Rev. C **74**, 025808 (2006).
- [34] S.-H. Shen, J.-N. Hu, H.-Z. Liang, J. Meng, P. Ring, and S.-Q. Zhang, Chin. Phys. Lett. **33**, 102103 (2016).
- [35] H. Tong, X.-L. Ren, P. Ring, S.-H. Shen, S.-B. Wang, and J. Meng, Phys. Rev. C **98**, 054302 (2018).
- [36] P. B. Demorest, T. Pennucci, S. M. Ransom, M. S. E. Roberts, and J. W. T. Hessels, Nature **467**, 1081 (2010).
- [37] J. Antoniadis *et al.*, Science **340**, 1233232 (2013).
- [38] M. Dutra, O. Lourenço, J. S. Sá Martins, A. Delfino, J. R. Stone, and P. D. Stevenson, Phys. Rev. C **85**, 035201 (2012).

- [39] M. Dutra, O. Lourenço, S. S. Avancini, B. V. Carlson, A. Delfino, D. P. Menezes, C. Providência, S. Typel, and J. R. Stone, *Phys. Rev. C* **90**, 055203 (2014).
- [40] W.-H. Long, N. V. Giai, and J. Meng, *Phys. Lett. B* **640**, 150 (2006).
- [41] A. Akmal, V. R. Pandharipande, and D. G. Ravenhall, *Phys. Rev. C* **58**, 1804 (1998).
- [42] E. Annala, T. Gorda, A. Kurkela, and A. Vuorinen, *Phys. Rev. Lett.* **120**, 172703 (2018).
- [43] B.-A. Li and A. W. Steiner, *Phys. Lett. B* **642**, 436 (2006).
- [44] J. M. Lattimer and M. Prakash, *Phys. Rep.* **333**, 121 (2000).
- [45] S. Gandolfi, J. Carlson, and S. Reddy, *Phys. Rev. C* **85**, 032801 (2012).
- [46] M. Baldo and G. F. Burgio, *Prog. Part. Nucl. Phys.* **91**, 203 (2016).
- [47] A. W. Steiner, J. M. Lattimer, and E. F. Brown, *Astrophys. J.* **722**, 33 (2010).
- [48] S. Bogdanov, C. O. Heinke, F. Özel, and T. Güver, *Astrophys. J.* **831**, 184 (2016).
- [49] M. B. Tsang, Y. Zhang, P. Danielewicz, M. Famiano, Z. Li, W. G. Lynch, and A. W. Steiner, *Phys. Rev. Lett.* **102**, 122701 (2009).
- [50] B.-A. Li, L.-W. Chen, and C. M. Ko, *Phys. Rep.* **464**, 113 (2008).
- [51] P. Russotto *et al.*, *Phys. Rev. C* **94**, 034608 (2016).